

A Model-Based Cross-Correlation Search for Gravitational Waves from Scorpius X-1

John T. Whelan¹, Santosh Sundaresan² and Prabath Peiris¹

¹Center for Computational Relativity & Gravitation Rochester Institute of Technology, Rochester, NY, USA;

²Indian Institute for Science Education and Research, Kolkata, India

john.whelan@astro.rit.edu

Gravitational Waves from LMXBs



Figure 1: Artist's impression of a low-mass X-ray binary. From *Astronomical Illustrations and Space Art*, by Fahad Sulehria, <http://www.novacelestia.com/>

A low-mass X-ray binary is a binary of a compact object (neutron star or black hole) & a companion star. If the CO is a NS, accretion from the companion can produce a hot spot & power GW emission from the non-axisymmetric NS. If GW spindown balances accretion spinup, GW strength can be estimated from X-ray flux, and GW freq \approx constant [1]. Sco X-1, the brightest LMXB, is thought to be a $1.4M_{\odot}$ NS + $0.42M_{\odot}$ companion [2]. Proposed & applied search methods include a fully coherent search over a small amount of data [3], an unmodelled search for a monochromatic stochastic signal [4], a search for a pattern of sidebands arising from the Doppler modulation of the signal by the binary orbit [5], and the modelled cross-correlation search described here [6]. These methods are currently being compared in a Mock Data Challenge; see poster C2.34.

Cross-Correlation Method

- Divide data into segments of length T_{sft} & take "short Fourier transform" (SFT) $\tilde{x}_I(f)$.
- Label segments by I, J, \dots (I & J can be same or different times or detectors) & pairs by α, β, \dots
- Use CW signal model ($\mathcal{A}_+ = \frac{1+\cos^2\iota}{2}$; $\mathcal{A}_\times = \cos\iota$)

$$h(t) = h_0 [\mathcal{A}_+ \cos\Phi(\tau(t))F_+ + \mathcal{A}_\times \sin\Phi(\tau(t))F_\times]$$

- expected cross-correlation between SFTs I & J

$$E[\tilde{x}_I^*(f_k) \tilde{x}_J(f_{k'})] = \tilde{h}_I^*(f_k) \tilde{h}_J(f_{k'}) = h_0^2 \tilde{\mathcal{G}}_{IJ} \delta_{T_{\text{sft}}}(f_k - f_{k'}) \delta_{T_{\text{sft}}}(f_{k'} - f_k)$$

- f_j is signal freq @ time T_j
Doppler shifted for detector I
- $\delta_{T_{\text{sft}}}(f - f') = \int_{-T_{\text{sft}}/2}^{T_{\text{sft}}/2} e^{i2\pi(f-f')t} dt$ so $\delta_{T_{\text{sft}}}(0) = T_{\text{sft}}$.

- Construct $\mathcal{Y}_{IJ} = \frac{\tilde{x}_I^*(f_k) \tilde{x}_J(f_{k'})}{(T_{\text{sft}})^2}$ (where $f_{k'} \approx f_k$) s.t.

$$E[\mathcal{Y}_{\alpha}] \approx h_0^2 \tilde{\mathcal{G}}_{\alpha} \quad \text{Var}[\mathcal{Y}_{IJ}] \approx \sigma_{IJ}^2 = \frac{S_I(f_0) S_J(f_0)}{4(T_{\text{sft}})^2}$$

- Optimally combine into $\rho = \sum_{\alpha} (u_{\alpha} \mathcal{Y}_{\alpha} + u_{\alpha}^* \mathcal{Y}_{\alpha}^*)$ w/ $u_{\alpha} \propto \frac{\tilde{\mathcal{G}}_{\alpha}^*}{\sigma_{\alpha}^2}$
so $E[\rho] = h_0^2 \sqrt{2 \sum_{\alpha} |\tilde{\mathcal{G}}_{\alpha}|^2 / \sigma_{\alpha}^2}$ & $\text{Var}[\rho] = 1$

Computational considerations limit coherent integration time. Can make tunable semi-coherent search by restricting which SFT pairs α are included in $\rho = \sum_{\alpha} (u_{\alpha} \mathcal{Y}_{\alpha} + u_{\alpha}^* \mathcal{Y}_{\alpha}^*)$. E.g., only include pairs where $|T_I - T_J| \equiv |T_{\alpha}| \leq T_{\text{max}}$

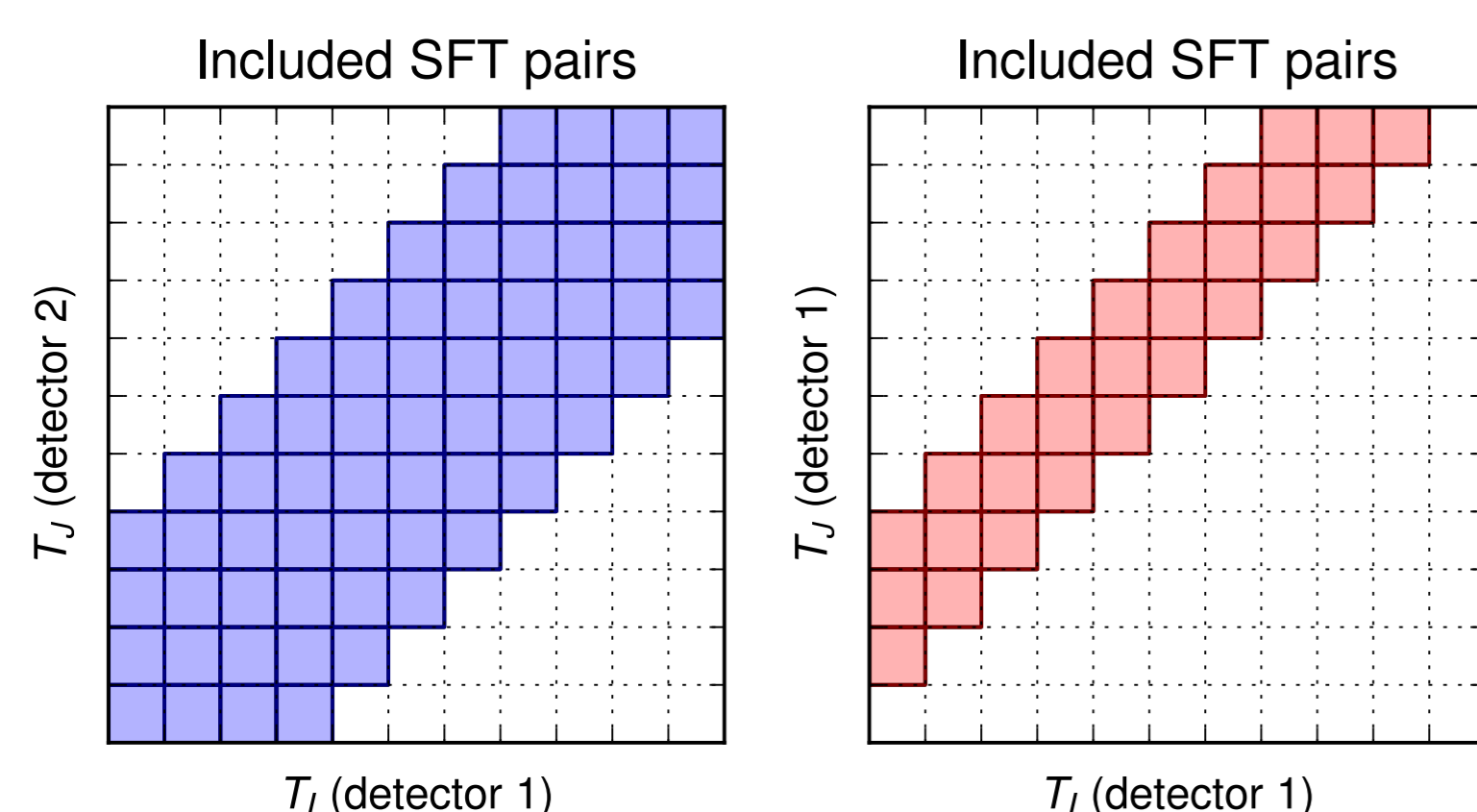


Figure 2: SFT pairs for inclusion in sliding cross-correlation search. Left: data from different detectors at same or different times. Right: data from same detector at different times. In this illustrative example, $T_{\text{max}} = 3T_{\text{sft}}$.

Parameter Space Metric

Consider dependence of ρ on parameters $\lambda \equiv \{\lambda_j\}$. Can define Parameter space metric via

$$\frac{E[\rho] - E[\rho^{\text{true}}]}{E[\rho^{\text{true}}]} = -g_{ij}(\Delta\lambda^i)(\Delta\lambda^j) + \mathcal{O}([\Delta\lambda]^3)$$

$$g_{ij} = -\frac{1}{2} \frac{E[\rho, ij]_{\lambda=\lambda^{\text{true}}}}{E[\rho^{\text{true}}]}$$

Assume dominant contribution to $E[\rho, ij]$ is from variation of $\Delta\Phi_{IJ} = \Phi_I - \Phi_J$; get phase metric

$$g_{ij} = \frac{1}{2} \frac{\sum_{\alpha} \Delta\Phi_{\alpha, i} \Delta\Phi_{\alpha, j} |\tilde{\mathcal{G}}_{\alpha}|^2 / \sigma_{\alpha}^2}{\sum_{\beta} |\tilde{\mathcal{G}}_{\beta}|^2 / \sigma_{\beta}^2} \equiv \frac{1}{2} \langle \Delta\Phi_{\alpha, i} \Delta\Phi_{\alpha, j} \rangle_{\alpha}$$

Note $\langle \rangle_{\alpha}$ is average over pairs weighted by $|\tilde{\mathcal{G}}_{\alpha}|^2 / \sigma_{\alpha}^2$; ignoring weighting factor would give usual metric [7]

$$\langle \Phi_{I, i} \Phi_{I, j} \rangle_I - \langle \Phi_{I, i} \rangle_I \langle \Phi_{I, j} \rangle_I$$

Define $T_{IJ} = T_I - T_J \equiv T_{\alpha}$ as time offset between SFTs; T_{α}^{av} is average time. For each detector pair, avg over pairs is avg over T_{α} & T_{α}^{av} . If we assume the avg over T_{α}^{av} evenly samples orbital phase, the metric in parameters f_0 (signal frequency), a_p (orbit radius projected along line of sight), \tilde{T} (time orbit crosses reference point) & P_{orb} (orbit period) is approximately diagonal, with

$$g_{f_0 f_0} \approx 2\pi^2 \langle T_{\alpha}^2 \rangle_{\alpha} \quad g_{P_{\text{orb}} P_{\text{orb}}} = \frac{4\pi^4 f_0^2 a_p^2 \sigma_T^2}{P_{\text{orb}}^4} \langle \sin^2 \frac{\pi T_{\alpha}}{P_{\text{orb}}} \rangle_{\alpha}$$

$$g_{a_p a_p} = \pi^2 f_0^2 \langle \sin^2 \frac{\pi T_{\alpha}}{P_{\text{orb}}} \rangle_{\alpha} \quad g_{\tilde{T} \tilde{T}} = \frac{4\pi^4 f_0^2 a_p^2}{P_{\text{orb}}^2} \langle \sin^2 \frac{\pi T_{\alpha}}{P_{\text{orb}}} \rangle_{\alpha}$$

(For reasonable values of $\sigma_T \sim$ observation time, $g_{P_{\text{orb}} P_{\text{orb}}}$ is small enough that we don't need to search over P_{orb} .)

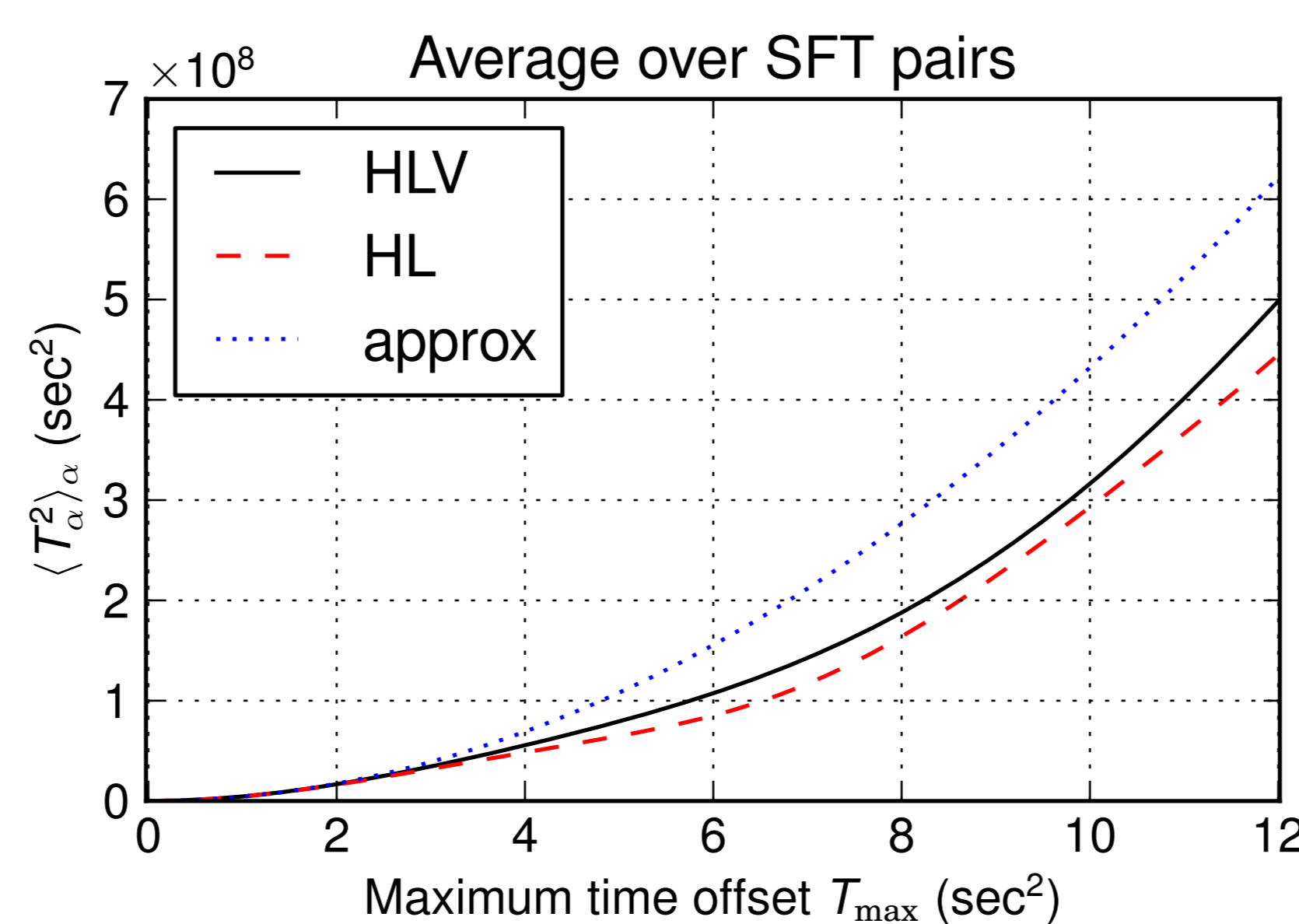


Figure 3: Factor $\langle T_{\alpha}^2 \rangle_{\alpha}$ appearing in metric element $g_{f_0 f_0}$. The metric is slightly over-estimated if geometry factors are ignored, relative to actual calculations for Hanford-Livingston (HL) and Hanford-Livingston-Virgo (HLV) network. Behavior of factor $\langle \sin^2 \frac{\pi T_{\alpha}}{P_{\text{orb}}} \rangle_{\alpha}$ appearing in other metric components is similar.

The metric determines how large a lag time T_{max} can be allowed while keeping computing cost manageable.

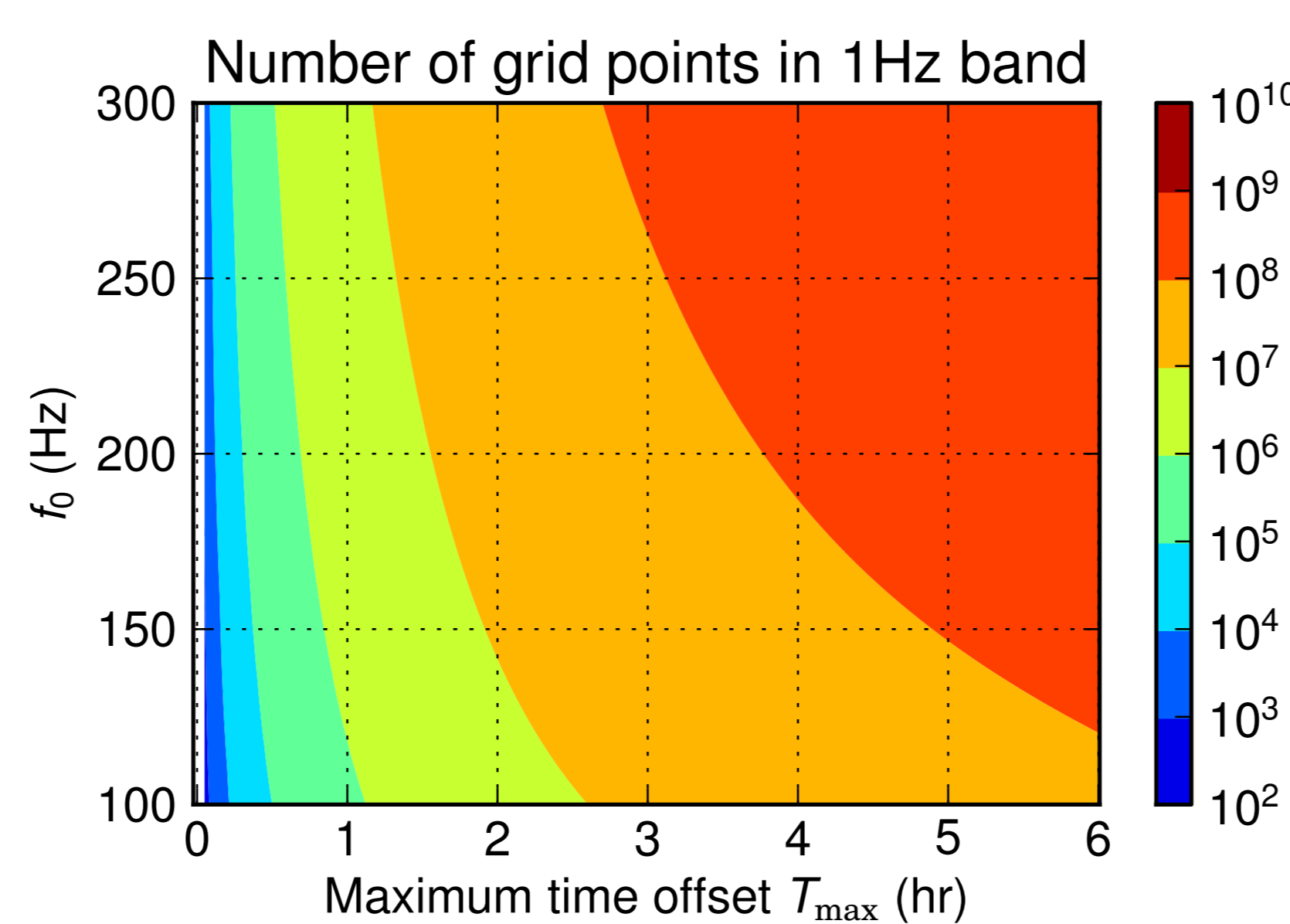


Figure 4: Number of templates needed for a search for GW from Sco X-1 at each frequency as a function of lag time. We allow a 20% mismatch and cover the one-sigma uncertainties in the parameters f_0 , a_p and \tilde{T} from [8].

Sensitivity Estimates

Search is sensitive to signal of amplitude

$$h_0 = \left(\frac{S^2}{\sum_{\alpha} |\tilde{\mathcal{G}}_{\alpha}|^2 / \sigma_{\alpha}^2} \right)^{1/2}$$

where S is a statistical factor. $\tilde{\mathcal{G}}_{\alpha}$ depends on (unknown) spin orientation angles ι & ψ ; standard approach is to average value of $\tilde{\mathcal{G}}_{\alpha}$ over $\cos\iota$ & ψ . The ψ effect is small after average over sidereal time. The ι effect means actually

$$E[\rho] \approx h_0^2 \frac{\mathcal{A}_+^2 + \mathcal{A}_\times^2}{2} \sqrt{2 \sum_{\alpha} |\tilde{\mathcal{G}}_{\alpha}|^2 / \sigma_{\alpha}^2}$$

Net effect is to change statistical factor S , which reduces the sensitivity of the search to h_0 by a factor of $\sqrt{S^{\text{eff}}/S}$.

	S			S^{eff}			$\sqrt{S^{\text{eff}}/S}$		
	FD			FD			FD		
FA	0.10	0.05	0.01	0.10	0.05	0.01	0.10	0.05	0.01
0.10	1.81	2.07	2.55	3.49	4.45	6.27	1.39	1.47	1.57
0.05	2.07	2.33	2.81	4.15	5.16	7.03	1.42	1.49	1.58
0.01	2.55	2.81	3.29	5.42	6.52	8.47	1.46	1.52	1.60

Table 1: Approximate modification of search sensitivity, as a function of desired false alarm probability and false dismissal probability, resulting from filtering with a template averaged over the signal parameters $\cos\iota$ and ψ . The detectable signal amplitude h_0 is proportional to $\sqrt{S^{\text{eff}}}$, so the sensitivity is reduced by the factor in the third group of columns. Note that the worst-case value for this is $\sqrt{16/5} \approx 1.79$

We illustrate the sensitivity of the search, and its dependence on the maximum allowed time lag T_{max} , using the advanced LIGO and Virgo design noise spectra from [9], and assuming a one-year observation. We plot the h_0 level that could be detected with 10% false-alarm and false-dismissal.

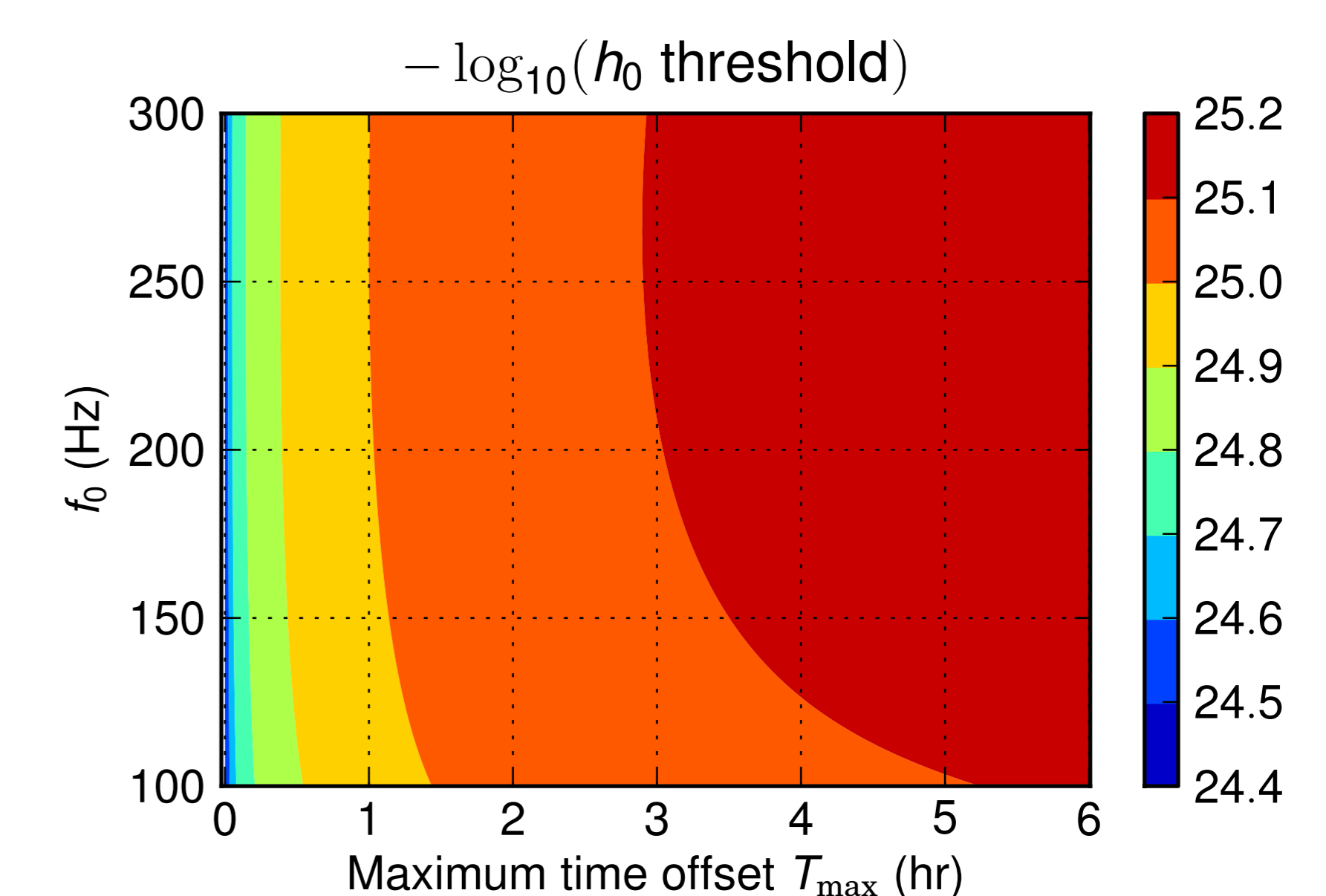


Figure 5: Sensitivity of a cross-correlation search for Sco X-1 with one year of advanced LIGO and Virgo design-sensitivity data, assuming 10% false-alarm & dismissal. Note that the $T_{\text{max}} = 0$ measurement is effectively the directed stochastic "radiometer" search.

References

- [1] Bildsten, *ApJL* **501**, L89 (1998)
- [2] Steeghs & Casares *ApJ* **568**, 273 (2002)
- [3] LSC, *PRD* **76**, 082001 (2007)
- [4] Ballmer, *CQG* **23**, S179 (2006)
LSC, *PRD* **76**, 082003 (2007)
- [5] Messenger & Woan, *CQG* **24**, S469 (2007)
- [6] Dhurandhar et al, *PRD* **77**, 082001 (2008)
- [7] Pletsch, *PRD* **82**, 042002 (2010)
- [8] Galloway et al in preparation
- [9] LSC & Virgo, [arXiv:1304.0670](https://dcc.ligo.org/LIGO-P1200087-v18/public)
<https://dcc.ligo.org/LIGO-P1200087-v18/public>